

## Fabrication of Fully Dense UHTC by Combining SHS and SPS

C. Musa, R. Licheri, R. Orrù\*, G. Cao

Dipartimento di Ingegneria Meccanica, Chimica e dei Materiali, Centro Studi sulle Reazioni Autopropaganti (CESRA), Unità di Ricerca del Consorzio Interuniversitario Nazionale per la Scienza e Tecnologia dei Materiali (INSTM), Piazza d'Armi, 09123 Cagliari, Italy

### Abstract

The combination of the Self-propagating High-temperature Synthesis (SHS) technique and the Spark Plasma Sintering (SPS) technology is adopted in this work for the fabrication of fully dense MB<sub>2</sub>-SiC and MB<sub>2</sub>-MC-SiC (M = Zr, Hf, Ta) Ultra High Temperature Ceramics (UHTCs). Specifically, Zr, Hf or Ta, B<sub>4</sub>C, Si, and graphite reactants are first converted to the desired composites by SHS. For the case of the low-exothermic Ta-based compositions, a preliminary 20 min ball milling treatment of the starting reactants is required to activate the corresponding synthesis reactions.

When the resulting powders are then subjected to consolidation by SPS, it is found that products with relative densities greater than 96% can be obtained for all systems investigated within 30 min of total processing time, when setting the dwell temperature to 1800 °C and the mechanical pressure to 20 MPa.

Hardness, fracture toughness, and oxidation resistance characteristics of the resulting dense UHTCs are comparable to, or superior than, those relative to similar products synthesized by alternative, less rapid, processing routes.

Moreover, it is found that the ternary composites display relatively low resistance to oxidation as a consequence of the lower SiC content in the composite, in comparison with the binary systems, as well as to the presence of transition metal carbides. Indeed, although the latter ones are potentially able to increase mechanical and resistance to ablation properties, they tend to oxidize rapidly to form MO<sub>2</sub> and CO<sub>x</sub>, so that the resulting porosity make the material bulk more sensitive to oxidation.

### Introduction

The increasing interest in ceramic composites based on transition metal borides and carbides (MB<sub>2</sub> and MC, where M = Zr, Hf, Ta), often referred to as Ultra High Temperature Ceramics (UHTCs), is due to the combination of their interesting physical, thermal and mechanical properties, such as melting temperatures above 2700 °C, high hardness, high electrical and thermal conductivity, chemical inertness, good resistance to thermal shock and to ablation in oxidizing environments [1].

These characteristics make UHTCs suitable for several room- and high-temperature structural applications, like cutting tools, high temperature crucibles, microelectronics as well as in aerospace industry for the fabrication of thermal protection components [1-3]. The intrinsic properties of MB<sub>2</sub> and MC materials can be further improved through the introduction of suitable additional phases. For instance, it is well established that the addition of cer-

tain Si-containing compounds, particularly SiC, is highly beneficial to increase the oxidation resistance at high temperatures of this class of ceramics [4-7].

The fabrication of dense UHTCs is generally attained by Hot Pressing (HP), through which ceramic powders are sintered at high temperature and in presence of mechanical loads [5, 8]. Alternatively, the HP method can be adopted to perform the material synthesis and consolidation in a single processing step using appropriate reactants [9-10]. The main drawbacks encountered when following the HP approach to produce dense refractory ceramics are represented by the excessively high temperatures and, above all, prolonged processing times, generally on the order of hours. In addition, under these operating conditions, materials with coarse microstructure are typically obtained. One of the possible solution proposed to improve the intrinsically low sintering ability of UHTCs is based on the use of sintering aids like Si<sub>3</sub>N<sub>4</sub> [5] or MoSi<sub>2</sub> [11], etc., but the consolidation time still remains too high.

\* Corresponding author. E-mail: roberto.orrù@dimcm.unica.it

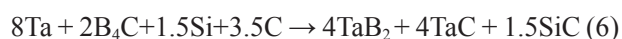
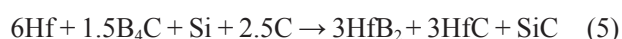
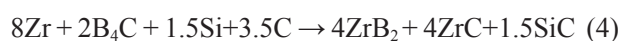
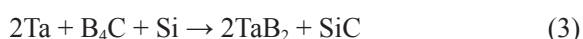
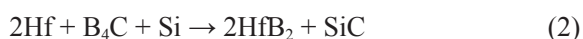
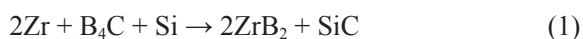
A different approach recently proposed to overcome the disadvantages outlined above makes use of the innovative Spark Plasma Sintering (SPS) technology, where the initial powders to be only densified or also simultaneously reacted are directly crossed by an electric pulsed current [12]. Several dense advanced materials with uniform and fine microstructure are obtained relatively faster and at lower temperature levels by SPS, with respect to HP. Among these materials, various UHTCs have been also prepared [7, 12-15].

The fabrication of dense ceramics could be also facilitated when starting from powders characterized by higher sintering ability. In this regard, the Self-propagating High-temperature Synthesis (SHS), a combustion synthesis method based on the occurrence of strongly exothermic reactions that, once ignited, auto-propagate in the form of a combustion wave through the reacting mixture [16-17] could provide a useful tool for the preparation of UHTC powders to be sintered by SPS. This combined approach was for instance successfully applied for the obtainment of several intermetallic compounds [18].

In this paper, the SHS and SPS processes are coupled to obtain highly dense MB<sub>2</sub>-SiC and MB<sub>2</sub>-MC-SiC (M = Zr, Hf, Ta) products starting from Zr/Hf/Ta, B<sub>4</sub>C, Si, and graphite powders. For the case of the low-exothermic TaB<sub>2</sub>-based system, the synthesis step is preceded by a high-energy ball milling treatment. The most influencing sintering parameters (dwell temperature and time) are optimized and the resulting bulk products are characterized from the mechanical and oxidation resistance points of view.

## Experimental

Zr (Alfa-Aesar, particle size < 44 μm, > 98.5% purity), Hf (Alfa-Aesar, < 44 μm particle size, > 99.6% purity), Ta (Alfa-Aesar, < 44 μm particle size, 99.9% purity), B<sub>4</sub>C (Alfa-Aesar, 1-7 μm particle size, > 99.4% purity), Si (Aldrich, < 44 μm particle size, > 9% purity) and graphite (Aldrich, 1-2 μm particle size) are used for the preparation of the different UHTC composites by SHS. Mixing of reactants was performed in agreement with the following reactions stoichiometry:



Accordingly, ZrB<sub>2</sub>-25 vol.% SiC (ZS), HfB<sub>2</sub>-26 vol.% SiC (HS), TaB<sub>2</sub>-27.9 vol.% SiC (TS), ZrB<sub>2</sub>-40 vol.% ZrC-12 vol.% SiC (ZZS), HfB<sub>2</sub>-40.6 vol.% HfC-11.2 vol.% SiC (HHS), and TaB<sub>2</sub>-39.1 vol.% TaC-13.7 vol.% SiC (TTS), respectively, are the expected products from the complete conversion of the initial reactants. It should be noted that the compositions above fall well within the ranges of volume percentage of higher resistance to ablation ceramic components [19], i.e. 20-64 vol.% MB<sub>2</sub>, 20-64 vol.% MC, and 10-16 vol.% SiC (M = Zr or Hf).

Powders mixing was performed in a SPEX 8000 (SPEX CertiPrep, USA) shaker mill for 30 min using plastic vials and alumina balls. Mechanochemical activation of Ta-based mixtures was carried out using the same mill apparatus with two steel balls (13 mm diameter, 8 grams weight) for 20 min milling time interval and ball to powders or charge ratio equal to 1. Details on the experimental set-up used in this work for SHS and SPS are described elsewhere [17, 20]. Depending upon the system investigated, a suitable amount (8-15 g) of the starting powders either unmilled (only mixed) or mechanochemically activated were uniaxially pressed to form cylindrical pellets with a diameter of 10 mm, height of 20-30 mm and a green density of 50-62% of the theoretical values. The combustion front was generated at one sample end by using an electrically heated tungsten coil, which was immediately turned off as soon as the synthesis reaction was initiated. Then, the reactive process self-propagated until the opposite end of the pellet was reached. The temperature during reaction evolution was measured using C-type thermocouples (W-Re, 127 μm diameter, Omega Engineering Inc., USA) as well as by a two-color pyrometer (IRCON, Mirage, USA). To convert the obtained SHS product to powder form, about 4 g of it were grinded by means of the shaker mill apparatus mentioned above, using a stainless steel vial with two steel balls (13 mm diameter, 8 g weight) for 20 min. Particle size distribution of the obtained powders was determined using a laser light scattering analyser (CILAS 1180, France).

An SPS 515 apparatus (Sumitomo Coal Mining Co. Ltd, Japan) was used in the temperature controlled mode for powder densification. This machine combines a 50 kN uniaxial press with a DC pulsed current generator (10 V, 1500 A, 300 Hz) to simultaneously provide a pulsed electric current through the sample and the graphite die containing it, and a mechanical load through the die plungers.

A certain amount (3-6 g) of the SHS powders was poured inside the die (outside diameter, 35 mm; inside diameter, 15 mm; height, 40 mm) and processed by SPS. Temperature, applied current and voltage, mechanical load and the vertical displace-

ment of the lower electrode were recorded in real time during sintering. In particular, temperature was measured by both a C-type thermocouple (Omega Engineering Inc., USA), which was inserted inside a small hole in one side of the graphite die, and a two-color pyrometer (IRCON, Mirage, USA). The measured displacement can be regarded as the degree of powdered compact densification, although thermal expansion of the sample, both electrodes, graphite blocks, spacers and plungers, also contribute to this parameter. Thus, a specific procedure was followed [20] to determine the sample shrinkage ( $\delta$ ).

The influence of the dwell temperature ( $T_D$ ) and total time ( $t_{SPS}$ ) was investigated while maintaining constant the applied pressure ( $P = 20$  MPa) and the non isothermal heating time ( $t_H$ ).

The relative densities of dense products were determined by the Archimedes' method. The theoretical density of the ZS, HS, TS, ZZS, HHS and TTS composites, i.e. 5.37, 9.13, 9.98, 6.02, 10.92, 12.05 g/cm<sup>3</sup>, respectively, were calculated through an appropriate rule of mixture [21] by considering the density values of ZrB<sub>2</sub>, HfB<sub>2</sub>, TaB<sub>2</sub>, ZrC, HfC, TaC, and SiC as 6.1, 11.18, 12.6, 6.4, 12.69, 14.48, and 3.2 g/cm<sup>3</sup>, respectively. Phase identification was performed by a Philips (The Netherlands) PW 1830 X-rays diffractometer using a Ni filtered Cu K<sub>α</sub> radiation ( $\lambda = 1.5405$  Å). The microstructure and local phase composition of end products were examined by SEM (mod. S4000, Hitachi, Japan) supported by EDS (Kevex Sigma 32 Probe, Noran Instruments, USA) analysis.

Vickers hardness (HV) and fracture toughness (KIC) of the SPSed products was performed using a Zwick 3212 Hardness tester machine (Zwick & Co. GmbH, Germany). The applied loads were in the range 1-10 kg while the dwell time was 18 s.

The oxidation resistance of UHTCs was determined by TGA (STA 409PC Simultaneous DTA-TGA Instrument, NETZSCH, Germany) under 100 mL/min air flow. Specifically, oxidation tests were conducted either under non-isothermal conditions by heating slowly (2 °C/min) the specimen from room temperature to 1450 °C or isothermally at 1450 °C for about 4 h, during which the mass sample variation with temperature and time, respectively, was monitored. For the sake of comparison, the obtained results have been normalized by dividing sample mass gain by the external surface of the UHTC material exposed to an oxidizing environment.

## Results and Discussion

Only ZrB<sub>2</sub>- and HfB<sub>2</sub>-based reacting systems were observed to display a self-propagating character upon ignition, when starting from simply

blended powder mixtures. In contrast, although consistently with the relatively lower enthalpies of reaction (Table 1), the TS and TTS compositions did not show an SHS behaviour. Thus, in the latter cases, the starting reactants have received a BM treatment to enhance system reactivity and promote the synthesis reactions (3) and (6).

**Table 1**

Enthalpy of formation ( $-\Delta H_f^\circ$ ) of UHTC composites according to reactions (1)-(6) [22] along with the corresponding combustion temperatures ( $T_c$ ) and average front velocities ( $v_f$ ) measured during SHS.

System	$-\Delta H_f^\circ$	$T_c$ [°C]	$v_f$ [mm/s]
ZS	647.3	2200 ± 20	11 ± 1
HS	674.0	2150 ± 50	7 ± 1
TS	348.4	1850 ± 50*	4.5 ± 0.5*
ZZS	2044.5	2200 ± 50	8 ± 1
HHS	1727.6	2250 ± 50	10 ± 1
TTS	1380.8	2000 ± 50*	5.7 ± 0.4*

\*starting reactants have received a ball-milling treatment

The combustion temperatures and the corresponding average front velocities measured during the SHS process evolution are also reported in Table 1. It is seen that relatively lower values are obtained for the less-exothermic TaB<sub>2</sub>-based systems.

The X-ray diffraction results relative to the SHS products are shown in Fig. 1(a)-1(f) along with those of the corresponding reactant mixtures. In addition, the XRD patterns of powders reactants after the mechanical treatment are also reported for the case of the TS and TTS systems. Other than a slight peaks broadening, as a manifestation of crystal size refinement and internal strain increase in the processing powders, no additional effects induced by BM can be evidenced from the XRD results. Nevertheless, it is clear that the mechanical treatment of the starting mixture favours interfaces formation among reactants, so that the original diffusion limitation can be overcome and system reactivity increased.

All the major peaks related to the phases constituent the desired ceramic composites are detected by XRD analysis of SHS products. It should be also noted that the secondary phases present as impurities in the as-received reactants when synthesizing ZrB<sub>2</sub>-based composites (Fig. 1(a)-1(b)), were completely eliminated (self-cleaning character of the SHS process) during synthesis occurrence. In conclusion, it is possible to state that a complete conversion of reactants into the expected composite phases is achieved by SHS for all systems investigated.

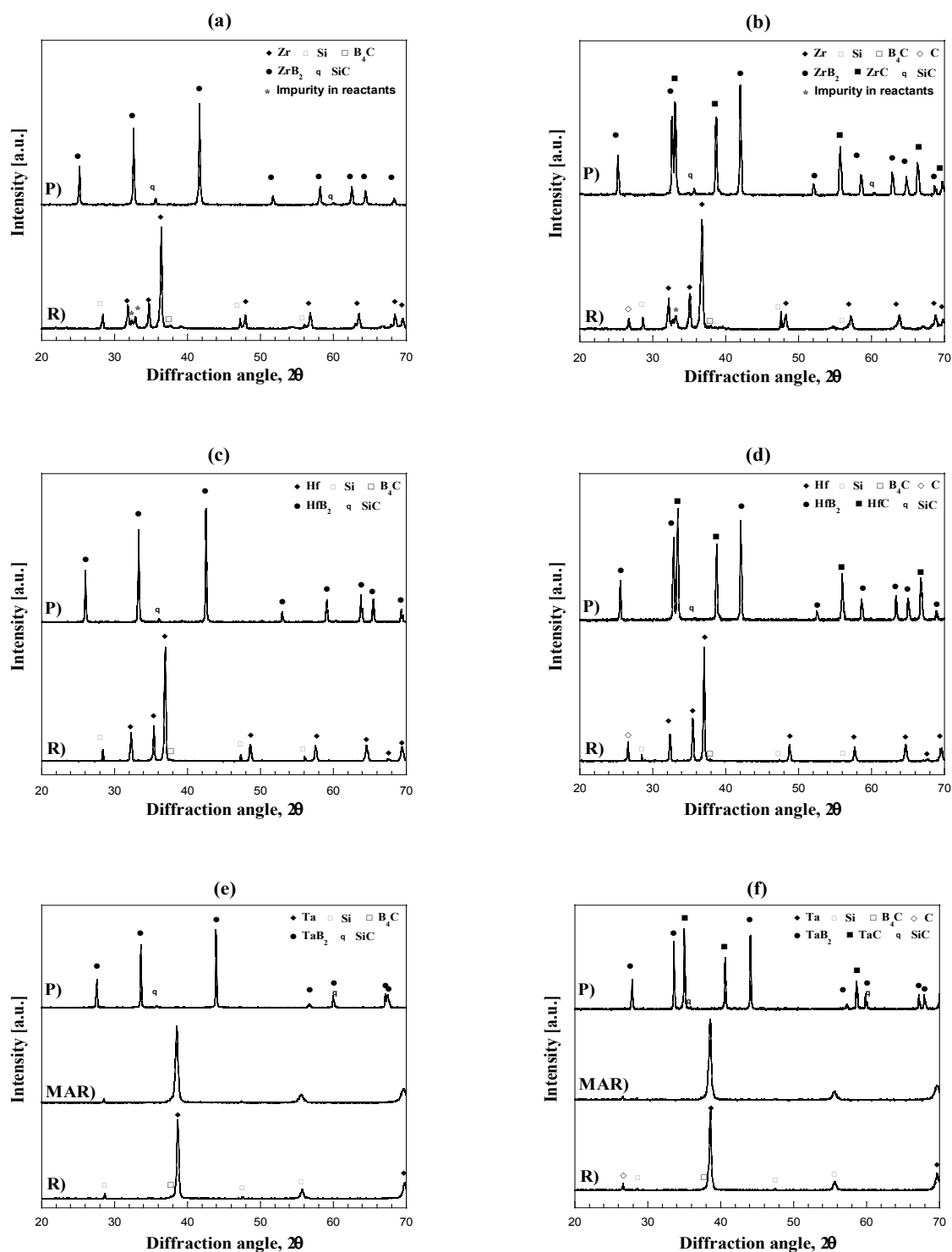


Fig. 1. Comparison of XRD patterns of R) original reactants, MAR) mechanochemically activated reactants and P) products obtained by self-propagating high-temperature synthesis according to reactions (1)-(6): (a) ZS, (b) ZZS, (c) HS, (d) HHS, (e) TS and (f) TTS.

The powders obtained after grinding for 20 min the SHS porous products have been characterized in terms of particle size distribution and microstructure. Specifically, particle size characteristics

obtained by laser light scattering analysis are summarized in Table 2. It is evidenced that powders are  $< 70 \mu\text{m}$  sized with  $d_{50}$  equal to few microns for all UHTCs.

**Table 2**

Particle size details of grinded SHSed products

System	Particle Size [ $\mu\text{m}$ ]	$d_{50}$ [ $\mu\text{m}$ ]
ZS	< 20	$2.51 \pm 0.02$
HS	< 30	$3.00 \pm 0.20$
TS	< 30	$1.19 \pm 0.09$
ZZS	< 70	$7.23 \pm 0.13$
HHS	< 40	$3.05 \pm 0.10$
TTS	< 40	$1.17 \pm 0.08$

SEM investigations conducted on powders samples are consistent with laser light scattering results. Three SEM back scattered micrographs representa-

tive of the ternary systems are shown in Figs. 2(a)-2(c). An analogous situation is encountered for the binary compositions. It is observed that each individual SHS powder particle typically consists of a mixture of MC (brighter),  $\text{MB}_2$  (medium bright), and SiC (darker) grains, each of them being typically less than 3-4  $\mu\text{m}$  in size. This analysis also evidences a relatively finer grained product for the case of TTS powders. This fact may be associated to the preliminary ball milling treatment received by the corresponding reactants for activating the SHS reaction, that apparently leads also to a microstructure refinement of the end product. In addition, the relatively low combustion temperatures (Table 1) achieved during the synthesis evolution as compared to the other UHTCs compositions are also responsible for the limitation of grain growth phenomena.

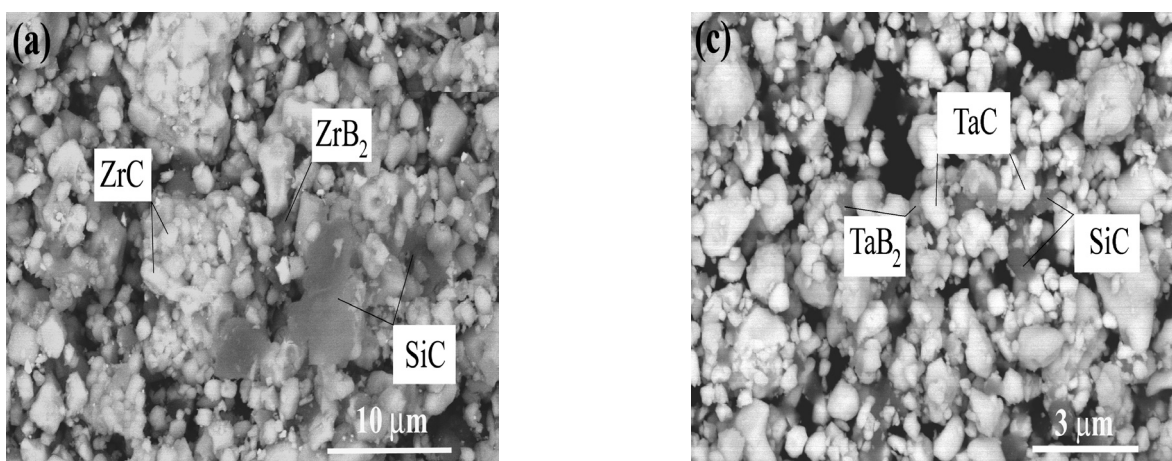


Fig. 2. SEM back-scattered micrographs of composite powders obtained by SHS: (a) ZZS, (b) HHS and (c) TTS.

Typical outputs of sample shrinkage ( $\delta$ ), expressed as a percentage relative to its final value, and temperature recorded during the consolidation process by SPS of HS powders are reported in Fig. 3(a). Specifically, they refer to the conditions of  $T_D = 800^\circ\text{C}$ ,  $t_H = 10$  min,  $t_{\text{SPS}} = 30$  min, and  $P = 20$  MPa. The corresponding current and voltage behaviour is shown in Fig. 3(b) where the electrical mean values are reported.

No peculiar changes in the sample shrinkage are manifested during the first 4 min of the SPS process (Fig. 3(a)). Subsequently,  $\delta$  increases at an approximately constant rate until the  $T_D$  value is reached. During the isothermal stage, densification continues to occur albeit at a minor rate to achieve final density ( $> 99.9\%$ ) at  $t_T = 30$  min. Regarding the electrical behaviour of the system (Fig. 3(b)), it may be seen that the current and voltage are augmented during the nonisothermal heating, to satisfy the chosen thermal program. Afterwards, both parameters rap-

idly decrease down to the corresponding stationary mean values, i.e. about 920 A and 4.6 V, respectively. Sample shrinkage, temperature, mean current and voltage time profiles recorded during the SPS process of the other UHTC powders investigated in this work were qualitatively similar to those obtained for the HS system and shown in Fig. 3(a)-3(b).

The influence of dwell temperature and the total SPS time was systematically studied and the obtained results are shown in Fig. 4(a)-4(b). Specifically, the effect of the first parameter was investigated for the ZS system in the range 1400-1800  $^\circ\text{C}$  for the case of the ZS system when the total processing time,  $t_{\text{SPS}}$ , was set to 20 or 30 min (Fig. 4(a)). As expected, as the dwell temperature is increased, residual porosity in the SPS product tends to disappear. Based on this study, the optimal SPS conditions to produce fully dense materials ( $> 99.5\%$ ) are  $T_D = 1600^\circ\text{C}$ ,  $t_{\text{SPS}} = 30$  min or  $T_D = 1800^\circ\text{C}$ ,  $t_{\text{SPS}} = 20$  min.

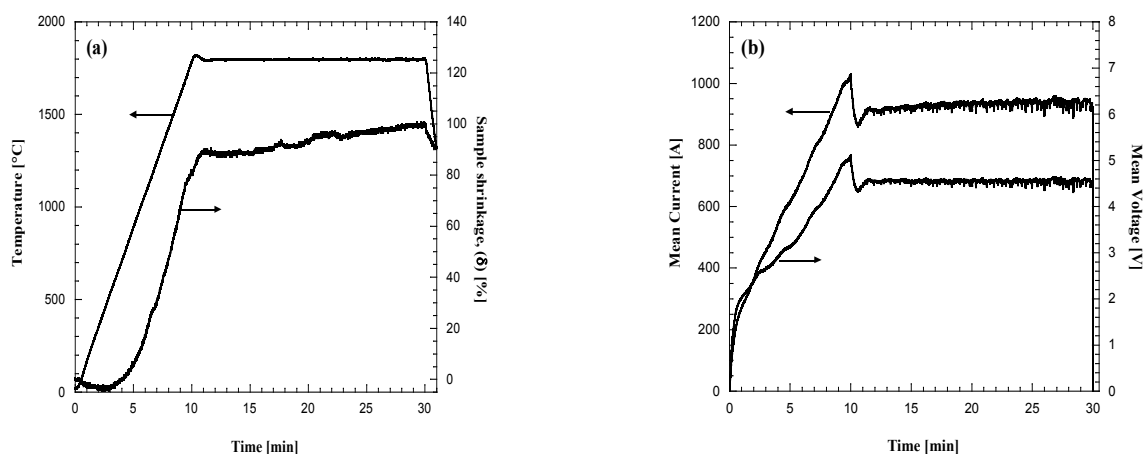


Fig. 3. Temporal profiles of SPS outputs during the preparation of dense HS products starting from powders obtained by SHS: (a) temperature and sample shrinkage, (b) mean current intensity and mean voltage ( $T_D = 1800$  °C,  $t_H = 10$  min,  $t_{SPS} = 30$  min,  $P = 20$  MPa).

Figure 4(b) shows the results obtained when investigating the effect of the sintering time on product density for the cases of HS and ZS compositions. It is observed that the average sample density at the end of the non-isothermal heating is less than 90% for both UHTCs. Higher density levels can be achieved only after isothermally heating the compact at  $T_D$  for 20 additional min. The major difficulty encountered when sintering the HS powders as compared to the ZS composition is due to the higher refractory nature of  $HfB_2$  with

respect to  $ZrB_2$  [1], as well as to the fact that the HS powders are relatively coarser (Table 2). In any case, near-fully dense bodies can be obtained for both materials within 30 min of total processing time. This holds also true when considering the other UHTCs taken into account in the present work. In conclusion, all bulk materials obtained under the SPS conditions of  $T_D = 1800$  °C,  $P = 20$  MPa, and  $t_{SPS} = 30$  min, were found to display relative densities  $\geq 96\%$  of the theoretical values.

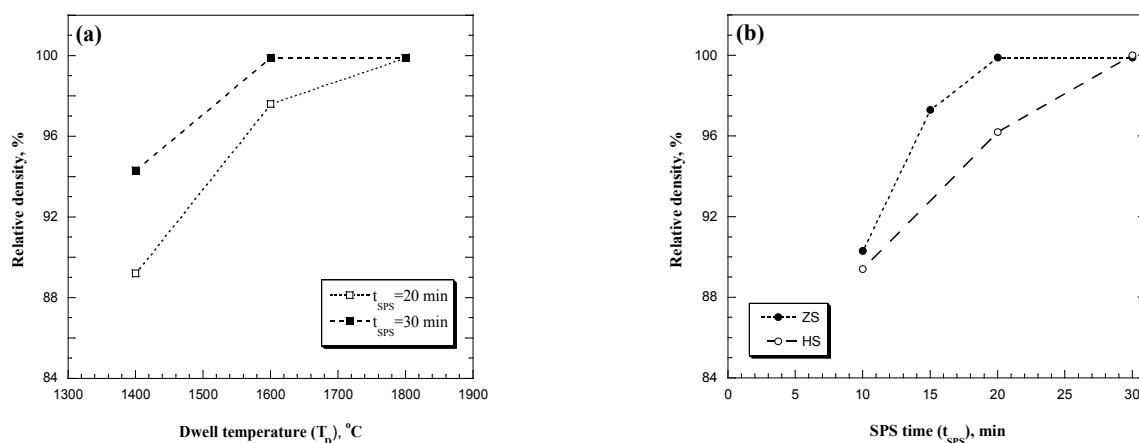


Fig. 4. Effect of (a) sintering temperature (ZS system) and (b) SPS time ( $T_D = 1800$  °C) on relative density of SPSed samples.

Three back-scattered SEM micrographs of the dense products obtained by SPS under the conditions  $T_D = 1800$  °C,  $P = 20$  MPa,  $t_H = 10$  min, and  $t_{SPS} = 30$  min, are shown in Figs. 5(a)-5(c) relatively

to the ternary composites. First of all, the obtainment of nearly fully dense materials is confirmed. In addition, the three expected ceramic phases, distributed quite uniformly all over the sample, are

easily distinguishable. Specifically, the darker, medium bright and brighter zones correspond to SiC, MB<sub>2</sub> and MC (M = Zr, Hf, Ta), respectively. It can be also observed that grain sizes are only slightly larger (generally less than 5 μm sized) with respect to the

starting SHS powders (Fig. 2(a)-2(b)). This outcome is a clear manifestation of the fact that the use of the SPS method avoids the occurrence of an excessive grain growth during the consolidation process.

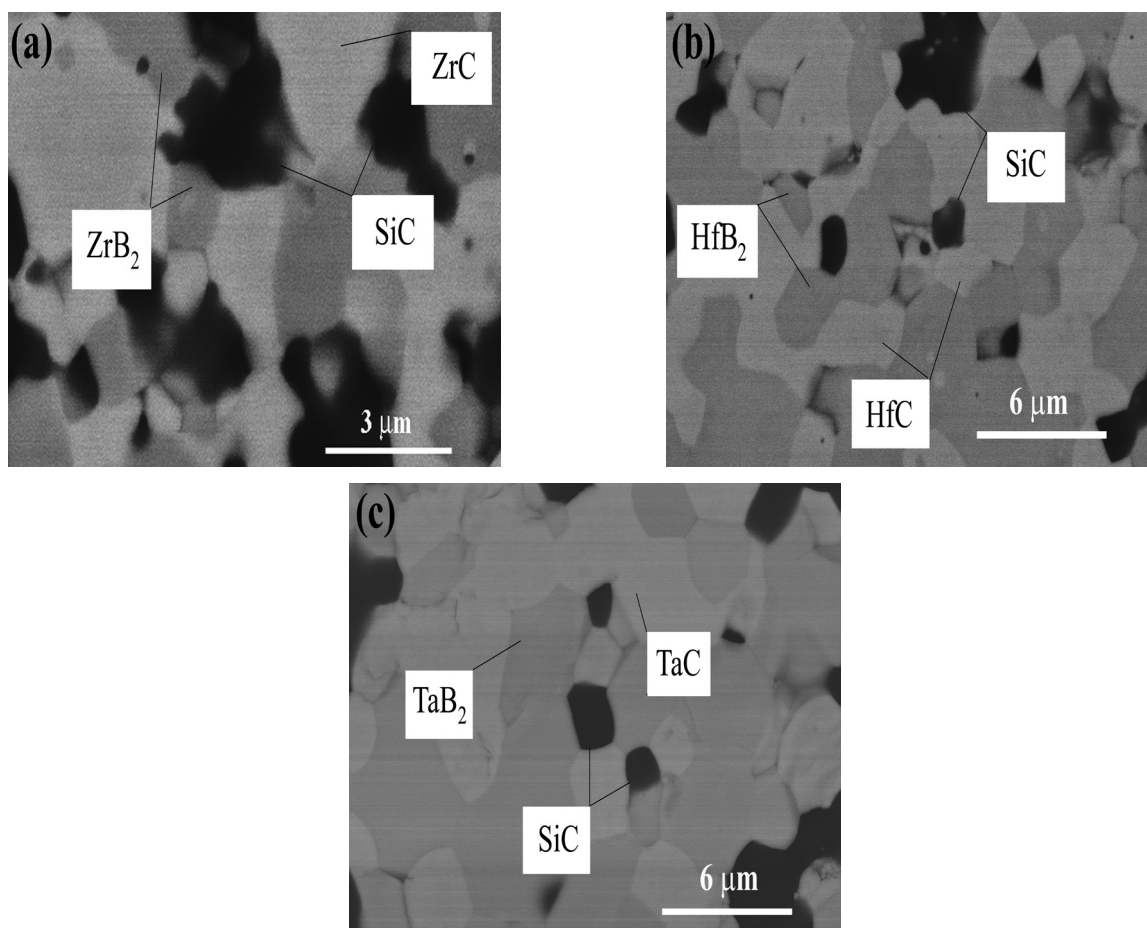


Fig. 5. SEM back-scattered micrographs of dense products obtained by SPS: (a) ZZS, (b) HHS and (c) TTS.

The measured Vickers hardness and fracture toughness properties of the SPSed UHTCs are reported in Table 3 along with the corresponding densities. The obtained data are comparable to, or better than, those ones reported in the literature relatively to similar compositions [23-24]. For example, the hot pressed fully dense HfB<sub>2</sub> - 20 vol.% SiC product [23] was reported to exhibit HV = 19-21 GPa and K<sub>IC</sub> = 4.1-4.2 MPa m<sup>1/2</sup>. Similarly, the ZrB<sub>2</sub> - 20 vol.% SiC and ZrB<sub>2</sub> - 6.4 vol.% ZrC - 20 vol.% SiC ceramics produced by reactive HP displayed HV = 13.6-16.7 GPa and K<sub>IC</sub> = 4.5-5.1 MPa m<sup>1/2</sup>, respectively [24]. The superior K<sub>IC</sub> values generally obtained in the present work, which provide an indication of material strength increase, can be readily ascribed to the more favorable sintering conditions encountered when processing SHS powders by SPS.

**Table 3**

Relative density ( $\rho$ ), Vickers hardness (HV) and fracture toughness (K<sub>IC</sub>) properties of the UHTC products sintered by SPS

System	$\rho$ [%]	HV [GPa]	K <sub>IC</sub> [MPa. <sup>1/2</sup> ]
ZC	99.6	HV1 = 16.7 ± 0.4	5.0 ± 0.3
HC	>99.9	HV10 = 19.2 ± 0.6	7.0 ± 0.7
TS	~96	HV10 = 18.9 ± 0.4	8.4 ± 0.8
ZZC	98.7	HV10 = 18.3 ± 1.1	5.9 ± 0.5
HHS	98.5	HV10 = 18.3 ± 1.1	6.2 ± 0.7
TTS	~96	HV10 = 18.3 ± 0.3	4.2 ± 0.3

Unfortunately, no information of mechanical properties related to compositions similar to TS and TTS systems could be found in the literature, so that the data reported for TaB<sub>2</sub> [3, 15], TaC and TaC-TaB<sub>2</sub> [25] products will be considered. Significantly high Vickers hardness (up to about 25 GPa) were obtained for the case of TaB<sub>2</sub> while the corresponding K<sub>IC</sub> values were  $4.5 \pm 0.3 \text{ MPa m}^{1/2}$  [3] or  $5.61 \pm 0.17 \text{ MPa m}^{1/2}$  [15]. Relatively modest mechanical properties were obtained for TaC (HV<sub>0.5</sub> =  $14.1 \pm 0.2 \text{ GPa}$  and  $K_{IC} = 3.5 \pm 0.2 \text{ MPa m}^{1/2}$ ) and TaC-TaB<sub>2</sub> ceramics ( $K_{IC} = 3.5 \pm 0.2 \text{ MPa m}^{1/2}$ ) [25]. Based on these results, it is clear that strong benefits for toughening UHTCs are provided by the presence of SiC.

The oxidation resistance of the composites prepared in this work has been measured using TGA by monitoring the mass change of the sample subjected to an oxidizing environment (air) at high temperatures. The results obtained during dynamic (non-isothermal) oxidation tests are reported in Fig. 6. It is seen that the binary systems exhibit higher resistance to oxidation as compared to the ternary composites. Among them, the HS ceramic displays the relatively lower oxidation rate up to 1450 °C. The same indication is provided by the oxidation tests conducted under isothermal conditions at 1450 °C. The observed oxidative behaviour can be explained on the basis of several studies reported in the literature on this subject [4, 6, 24]. Specifically, SiC oxidation leads to the formation of SiO<sub>2</sub> that could combine with the volatile B<sub>2</sub>O<sub>3</sub> specie, produced by the oxidation of MB<sub>2</sub>, to give a protective surface layer of silica-rich borosilicate glass. The latter one reduces boron evaporation, other than acting as an oxygen diffusion barrier, thus providing improvement of oxidation resistance of the UHTC material.

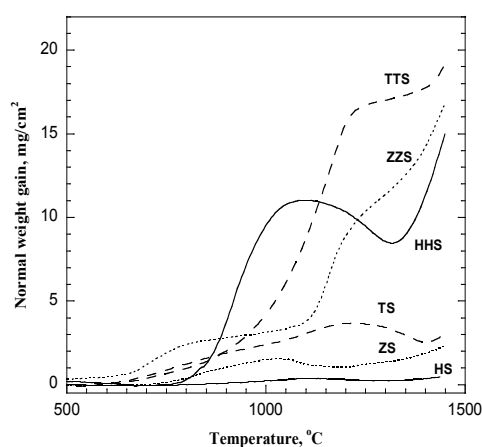


Fig. 6. Specific weight gain of the UHTC samples sintered by SPS as a function of temperature during TGA oxidation in air.

The relatively low resistance to oxidation displayed by the ternary systems can be associated to the lower SiC percentage present in these composite, with respect to the MB<sub>2</sub>-SiC materials, but also to the negative role played by MC in this regard. Indeed, although transition metal carbides are potentially able to increase mechanical and resistance to ablation properties, they oxidize rapidly to produce MO<sub>2</sub> and carbon oxides. Consequently, the resulting porous material permits the O<sub>2</sub> diffusion inside the bulk and, consequently, the progress of oxidation phenomena.

## Conclusions

The fabrication of nearly full dense binary and ternary UHTC composites was investigated in this work by combining the SHS and SPS techniques. Specifically, the powders to be consolidated by SPS were first obtained by SHS using Zr/Hf/Ta, B<sub>4</sub>C, Si, and, for the case of the ternary systems, graphite powders. The exploitation of such combustion synthesis route to rapidly produce the composite UHTC powders was made possible by the exothermic nature of the corresponding reactions. However, for the case of the TaB<sub>2</sub>-based composites, the mechanical activation of the initial reactants by ball milling for 20 min was needed to induce the SHS behaviour to the synthesis reactions. The complete conversion of reactants into the desired ceramic phases was achieved for all systems.

The powders obtained after grinding the SHS porous samples were subsequently consolidated by SPS without the addition of any sintering aid. The systematic investigation carried out to optimize the sintering process evidenced that  $\geq 96\%$  dense products can be obtained within 30 min of total processing time by setting a dwell temperature level equal to 1800 °C, P = 20 MPa, and a non-isothermal heating time of 10 min.

Vickers hardness, fracture toughness, and oxidation resistance properties of the obtained dense ceramics are generally similar to, and in some cases superior than, those related to analogous products fabricated by HP methods. Furthermore, the relatively shorter processing times and/or lower sintering temperature make the processing route adopted in this work preferable.

In this regard, a relevant contribution is also provided by the use of the SHS technique to synthesize in-situ the MB<sub>2</sub>-SiC and MB<sub>2</sub>-MC-SiC composite powders. This result is consistent with the higher sintering ability displayed by ZrB<sub>2</sub> powders prepared by combustion synthesis as compared to the analogous product obtained by the other techniques, i.e. replacement reaction and carbothermic reduc-



tion process [26]. Such behaviour was explained on the basis of the higher defect concentration observed in SHS products, as compared to the powders synthesized by other methods, as a consequence of the extreme heating and cooling conditions encountered during the rapid reaction front propagation. The same conclusion can be drawn when consolidating by SPS the ZrB<sub>2</sub>-ZrC-SiC powders obtained by SHS instead of taking advantage of relatively finer commercial powders with the same composition [12]. Indeed, relatively denser samples are correspondingly obtained in the first case.

Regarding the beneficial effects deriving by adopting the SPS technology, they can be ascribed to the advantages associated to the direct passage of the electric pulsed current through the sintering powders and the die containing them. This feature produces very high heating rates, so that processing times are significantly shortened and sintering temperatures lowered, with respect to conventional HP.

### Acknowledgments

IM (Innovative Materials) S.r.l., Italy, is gratefully acknowledged for granting the use of SPS apparatus. The authors thank Eng. Leonardo Esposito (Centro Ceramico di Bologna, Italy) for performing hardness and fracture toughness measurements.

### References

1. Fahrenholtz, W.G., Hilmas, G.E., Talmy, I.G., Zaykoski, J.A., Refractory diborides of Zirconium and Hafnium, *J. Am. Ceram. Soc.* 90: 1347-1364 (2007).
2. Levine, S.R., Opila, E.J., Halbig, M.C., Kiser, J.D., Singh, M., Salem, J.A., Evaluation of ultra-high temperature ceramics for aeropropulsion use, *J. Europ. Ceram. Soc.* 22: 2757-2767 (2003).
3. Zhang, X., Hilmas, G.E., Fahrenholtz, W.G., Synthesis, densification, and mechanical properties of TaB<sub>2</sub>, *Mater. Letters* 62: 4251-4255 (2008).
4. Hinze, J.W., Tripp, W.C., Graham, H.C., The High-Temperature Oxidation Behavior of HfB<sub>2</sub>+20 v/oSiC Composite, *J. Electrochem. Soc.* 122: 1249-1254 (1975).
5. Monteverde, F., Bellosi, A., The resistance to oxidation of an HfB<sub>2</sub>-SiC composite, *J. Eur. Ceram. Soc.* 25(7): 1025-1031 (2005).
6. Peng, F., Speyer, R.F., Oxidation resistance of fully dense ZrB<sub>2</sub> with SiC, TaB<sub>2</sub>, and TaSi<sub>2</sub> additives, *J. Am. Ceram. Soc.* 91: 1489-1494 (2008).
7. Musa, C., Orrù, R., Sciti, D., Silvestroni, L., Cao, G., Synthesis, consolidation and characterization of monolithic and SiC whiskers reinforced HfB<sub>2</sub> ceramics, *J. Europ. Ceram. Soc.* 33: 603-614 (2013).
8. Fahrenholtz, W.G., Hilmas, G.E., Chamberlain, A.L., Zimmermann, J.W., Fahrenholtz, B., Processing and characterization of ZrB<sub>2</sub>-based ultra-high temperature monolithic and fibrous monolithic ceramics, *J. Mater. Sci.* 39: 5951-5957 (2004).
9. Zhang, G.J., Deng, Z.Y., Kondo, N., Yang, J.F., Ohji, T., Reactive hot pressing of ZrB<sub>2</sub>-SiC-composites, *J. Am. Ceram. Soc.* 83: 2330-2332 (2000).
10. Monteverde, F., Progress in the fabrication of ultra-high-temperature ceramics: In situ synthesis, microstructure and properties of a reactive hot-pressed HfB<sub>2</sub>-SiC composite, *Compos. Sci. & Technol.*, 65: 1869-1879 (2005).
11. Balbo, A., Sciti, D., Spark Plasma Sintering and Hot Pressing of ZrB<sub>2</sub>-MoSi<sub>2</sub> under high temperature ceramics, *Mater. Sci. Eng. A*, 475: 108-112 (2008).
12. Orrù, R., Licheri, R., Locci, A.M., Cincotti, A., Cao, G., Consolidation/Synthesis of Materials by Electric Current Activated/Assisted Sintering, *Mater. Sci. Eng. R*, 63: 127-287 (2009).
13. Licheri, R., Orrù, R., Musa, C., Cao, G., Synthesis, densification and characterization of TaB<sub>2</sub>-SiC composites, *Ceram. Intern.* 36: 937-941 (2010).
14. Licheri, R., Orrù, R., Musa, C., Cao, G., Efficient technologies for the Fabrication of dense-TaB<sub>2</sub>-based Ultra High Temperature Ceramics, *ACS Appl. Mater. Interfaces* 2: 2206-2212 (2010).
15. Musa, C., Orrù, R., Licheri, R., Cao, G., Spark Plasma Synthesis and Densification of TaB<sub>2</sub> by Pulsed Electric Current Sintering, *Mater. Lett.* 65: 3080-3082 (2011).
16. Munir, Z.A., Anselmi-Tamburini, U., Self-propagating exothermic reactions: the synthesis of high-temperature materials by combustion, *Mater. Sci. Rep.* 3: 277-365 (1989).
17. Cincotti, A., Licheri, R., Locci, A.M., Orrù, R., Cao, G., A review on combustion synthesis of novel materials: recent experimental and modeling results, *J. Chem. Technol. Biot.* 78: 122-127 (2003).
18. Hirota, K., Nakane, S., Yoshinaka, M., Yamaguchi, O., Spark Plasma Sintering (SPS) of Several Intermetallic Compounds Prepared by Self-Propagating High-Temperature Synthesis (SHS), *Intern. J. SHS* 10: 345-358 (2001).
19. Bull, J., White, M.J., Kaufman, L., Ablation resistant Zirconium and Hafnium Ceramics, US Patent No. 5,750,450 (1998).

20. Locci, A.M., Orrù, R., Cao, G., Munir, Z.A., Simultaneous spark plasma synthesis and densification of TiC-TiB<sub>2</sub> composites, *J. Am. Ceram. Soc.* 89: 848-855 (2006).
21. Matthews, F.L., Rawlings, R., *Composite Materials: Engineering and Science*. Chapman & Hall, Great Britain (1994).
22. Barin, I., *Thermochemical data of pure substances*, VHC (1989).
23. Gasch, M., Ellerby, D., Irby, E., Beckman, S., Gusman, M., Johnson, S., Processing, properties and arc jet oxidation of hafnium diboride/silicon carbide ultra high temperature ceramics, *J. Mater. Sci.* 39: 5925-5937 (2004).
24. Wu, W.W., Zhang, G.J., Kann, Y.M., Wang, P.L., Reactive Hot Pressing of ZrB<sub>2</sub>-SiC-ZrC Ultra High-Temperature Ceramics at 1800 °C, *J. Am. Ceram. Soc.* 89: 2967-2969 (2006).
25. Zhang, X., Hilmas, G., Fahrenholtz, W.G., Densification, mechanical properties, and oxidation resistance of TaC-TaB<sub>2</sub> ceramics, *J. Am. Ceram. Soc.* 91: 4129-4132 (2008).
27. Mishra S.K., Das, S., Pathak, L.C., Defect structures in zirconium diboride powder prepared by self-propagating high-temperature synthesis, *Mater. Sci. Eng. A* 364: 249-255 (2004).

*Received 5 March 2013*